aP2-Cre-mediated inactivation of acetyl-CoA carboxylase 1 causes growth retardation and reduced lipid accumulation in adipose tissues

Jianqiang Mao[a], Tao Yang[b], Ziwei Gu[a], William C. Heird[c], Milton J. Finegold[d], Brendan Lee[b,e], and Salih J. Wakil[a,1]

[a]Verna and Marrs McLean Department of Biochemistry and Molecular Biology, [b]Department of Molecular and Human Genetics, [c]Department of Pediatrics-Children's Nutrition Research Center, [d]Department of Pathology, and [e]Howard Hughes Medical Institute, Baylor College of Medicine, One Baylor Plaza, Houston, TX 77030

Contributed by Salih J. Wakil, August 21, 2009 (sent for review April 28, 2009)

Adipose tissue is one of the major sites for fatty acid synthesis and lipid storage. We generated adipose (fat)-specific ACC1 knockout (FACC1KO) mice using the aP2-Cre/loxP system. FACC1KO mice showed prenatal growth retardation; after weaning, however, their weight gain was comparable to that of wild-type (WT) mice on a normal diet. Under lipogenic conditions of fasting/re-feeding a fat-free diet, lipid accumulation in adipose tissues of FACC1KO mice was significantly decreased; this is consistent with a 50–66% reduction in the ACC activity in these tissues compared with that of WT mice. Surprisingly, FACC1KO mice manifested skeletal growth retardation phenotype accompanied by decreased chondrocyte proliferation in the growth plate and lower trabecular bone density. In addition, there was about a 30% decrease in serum insulin-like growth factor I (IGF1), and while the serum leptin level was decreased by about 50%, it did not counteract the osteopenic effects of IGF1 on the bone. Fatty acid analyses of mutant bone lipids revealed relatively higher levels of C18:2n-6 and C18:3n-3 and lower levels of their elongation C20 homologs than that of WT cohorts, leading to lower levels of C20 homologs and bone development. Moreover, aP2-Cre-mediated ACC1 inactivation in bone tissue led to a decreased number of osteoblasts but not of osteoclasts. The downregulation of ACC1 on osteoblastogenesis may be the cause for the osteopenia phenotype of FACC1KO bone homeostasis.

fat-specific ACC1 knockout | osteoblastogenesis

Acetyl-CoA carboxylase 1 (ACC1) catalyzes the synthesis of malonyl-CoA, the committed step toward de novo synthesis of long-chain fatty acids from acetyl-CoA (1). Deletion of ACC1 in mice resulted in embryonic lethality, indicating that fatty acid synthesis is essential for embryonic development (2). To understand the importance of de novo fatty acid synthesis and the role of ACC1 in adult mouse tissues, we generated tissue-specific knockout mice using the Cre-loxP system (3). Mice with liver-specific knockout of ACC1 (LACC1KO) fed normal chow did not exhibit any significant physiological differences from wild-type (WT) mice (3). But when fed a fat-free diet, they accumulated significantly less triglyceride (TG) in the liver compared with their WT cohorts. Although inactivation of ACC1 resulted in 70–75% lower ACC activity in the liver, it did not affect either glucose homeostasis or hepatic fatty acid oxidation (3). When the LACC1KO mice were fed a fat-free diet for 10 days, there was an upregulation of PPARγ and several lipogenic enzymes in the liver, including a 2-fold increase in fatty acid synthase (FAS) mRNA, protein, and activity. However, syntheses of fatty acid and TG were reduced significantly. Upregulated ACC2 gene expression did not compensate for the loss of ACC1 function, an observation similar to that noted in Acc2$^{-/-}$ mice in which the cytosolic ACC1 did not compensate for the mitochondrial-associated ACC2 and its product malonyl-CoA (4).

Adipose tissues are active lipogenic and fat storage tissues, and white adipose is an important endocrine tissue secreting critical hormones and factors such as leptin, adiponectin, and TNF-α (5). The role of ACC1 in adipose function and energy homeostasis is still unknown. To identify the role of ACC1 in adipose tissue, we generated adipose (fat)-specific ACC1 knockout (FACC1KO) mice by breeding ACC1$^{lox/lox}$ mice with aP2-Cre mice (6). Expression of Cre was driven by the adipocyte protein 2 (aP2)-fatty acid binding protein 4 (FABP4) promoter, which is active predominantly in adipose tissue. We were surprised to find that FACC1KO mice showed prenatal growth retardation with impaired bone development, revealing a function of ACC1 in bone homeostasis.

Results

The generation of the floxed ACC1 allele-containing mice has been described earlier (3). The mice (ACC1$^{lox/lox}$ or lox$^{+/+}$) were bred with aP2-Cre mice (6) to disrupt ACC1 expression in adipose tissue. ACC1 exons were numbered according to the assumption that the first codon is located in exon 5, which is highly conserved among ACC1 genes in mammalians including human (7–11). Two loxP sites were positioned to flank ACC1 exon 22, which encodes the biotin-binding domain containing the -Met-Lys-Met- motif. The aP2-Cre^{+}/lox$^{+/-}$ mice were interbred to generate aP2-Cre^{+}/lox$^{+/+}$ mice as adipose (fat)-specific ACC1 knockout (FACC1KO) mice; the aP2-Cre^{-}/lox$^{+/+}$ mice were used as WT controls. Adipose-specific rearrangement of the ACC1 gene in the presence of the floxed locus and aP2-Cre was confirmed by RT-PCR analyses using primers derived from exons 21 and 24, a 299-bp fragment indicating the deletion of 135-bp exon 22 in white adipose tissue (WAT) and in interscapular brown adipose tissue (BAT) but not in liver (Fig. 1*A*). ACC1 gene rearrangement also occurred in the peritoneal macrophages (Mϕ) and bone marrow (BM), but the efficiency of Cre was less than that in the adipose (Fig. 1*A*). The DNA fragment, 299 bp, was not detected in the corresponding tissues of the WT mice (Fig. 1*A Lower*). qRT-PCR measurements show that the efficiency of deletion of the ACC1 exon 22 is about 50–85% in mutant mouse adipose tissue. These values compare well with the loss of >60% ACC activities in the white and brown adipose tissue of FACC1KO mice (Fig. 2*B*).

The food intake of WT mice and mutant mice was similar (4.1 ± 0.1 g/day vs. 4.2 ± 0.2 g/day per mouse, $P = 0.69$). But the most apparent phenotype of FACC1KO mice is prenatal growth retardation; this is evident after birth in body length and body weight, and becomes distinct at weaning age; 3-week-old male

Author contributions: J.M. and S.J.W. designed research; J.M., T.Y., Z.G., W.C.H., M.J.F., and B.L. performed research; Z.G., W.C.H., and M.J.F. contributed new reagents/analytic tools; J.M., T.Y., W.C.H., M.J.F., B.L., and S.J.W. analyzed data; and J.M., B.L., and S.J.W. wrote the paper.

The authors declare no conflict of interest.

[1]To whom correspondence should be addressed. E-mail: swakil@bcm.edu.

This article contains supporting information online at www.pnas.org/cgi/content/full/0909055106/DCSupplemental.

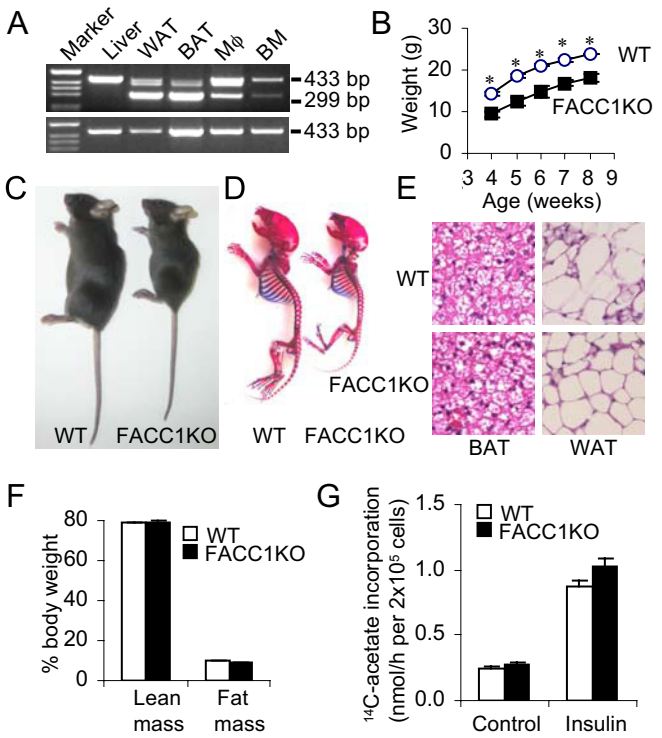

Fig. 1. Skeletal and adipocyte development. (*A*) RT-PCR analysis of total RNA from FACC1KO mice and WT mice using primers 21f/24r. (*Top* gel lanes) Marker, 1 kb DNA ladder; liver; WAT, white adipose tissue; BAT, interscapular brown adipose tissue; Mϕ, peritoneal macrophage; BM, bone marrow. Product (433-bp) represents the WT ACC1 gene. Product (299-bp) in mutant tissues—WAT, BAT, Mϕ, and BM—indicates the appropriate deletion of exon 22 in the ACC1 gene; this product was absent in the liver. *Bottom* gel shows the absence of the 229-bp band in the corresponding WT mouse tissues. (*B*) A typical growth curve for male mice ($n = 5$). *, $P < 0.005$. (*C*) Photographs of representative 4-week-old male WT and FACC1KO mice. (*D*) Skeleton of 7-day-old male mice from the same litter. The skeletons were stained with alcian blue for cartilage and with alizarin red for calcified tissues. (*E*) BAT and WAT from 4-week-old male WT and its FACC1KO littermate, were stained with hematoxylin and eosin (H&E). The original magnification, 160×. (*F*) Lean mass and fat mass in 7-week-old male mice ($n = 5$) using the dual-energy X-ray absorptiometry methods. Percentage of body weight is presented. (*G*) Lipogenesis in primary adipocytes from 3-month-old WT and FACC1KO mice ($n = 3$) in the absence (Control) or presence of 100 nM insulin.

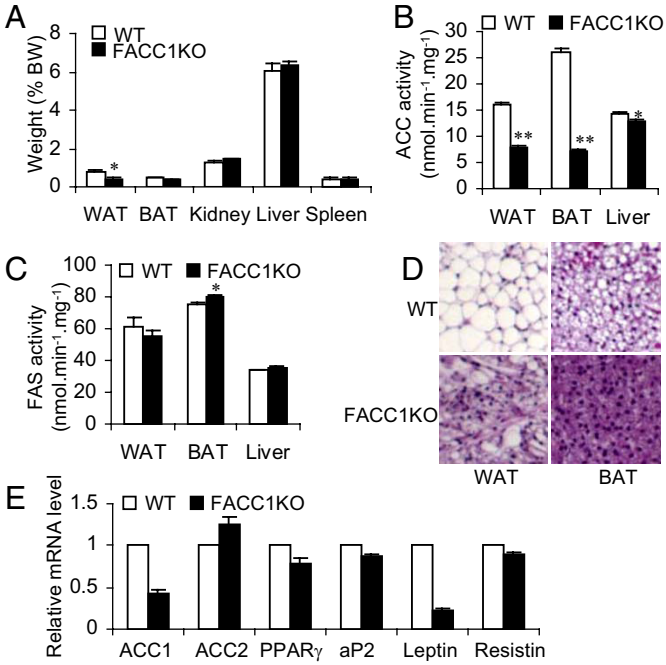

Fig. 2. ACC activities and lipid accumulation under lipogenic conditions of fasting and refeeding in tissues of FACC1KO mice. (*A*) Tissue weights expressed as percentages of body weight. WT mice and FACC1KO mice (15–16 weeks old, $n = 5$) were fasted for 2 days and then re-fed for 2 days with a fat-free diet to induce fat synthesis. *, $P < 0.05$. (*B* and *C*) The ACC and FAS activities in extracts of WAT, BAT, or livers partially purified with ammonium sulfate precipitation. *, $P < 0.05$; **, $P < 0.0001$. (*D*) H&E staining of adipose tissue sections show that FACC1KO mice accumulated less lipid in WAT and BAT than WT mice. The original magnification, 62×. (*E*) Real time PCR analyses of mRNA levels in WT mice and FACC1KO mice ($n = 4$).

FACC1KO mice weighed 33.5% less than their WT littermates (6.92 ± 0.23 g vs. 10.42 ± 0.25 g, $n = 9$–14, [$P < 0.0001$]). When fed normal chow, FACC1KO mice grew at a rate similar to that of WT mice (Fig. 1*B*). At 4 weeks of age, FACC1KO mice weighed approximately 30–40% less than WT mice (Fig. 1*C*). The skeletal preparation of 7-day-old FACC1KO mice showed overall shortening of all bone elements but with no overt patterning defect (Fig. 1*D*). Femur and tibia length in FACC1KO mice was approximately 15% shorter than in WT cohort mice.

The litter size and the ratio of FACC1KO mice to the total litter size—201 pups, 29 males and 28 females, in the first 28 litters (≈28%)—indicated that homozygous disruption of ACC1 in adipose tissue had no deleterious effect on embryonic development and survival; FACC1KO mice were normally fertile. However, the FACC1KO mice exhibit higher lethality around weaning age, 3 to 4 weeks old. While approximately 45% of the males (13 out of 29) and approximately 21% of the females (six out of 28) died, no WT pups died. Autopsies revealed that the dead FACC1KO mice had little or no body fat. The cause may have been their inability to nurse well because of their smaller size, or this group of mice may represent a different phenotype; further investigation is needed. The surviving mice have been studied in detail and are reported in this paper.

Histological analyses of WAT and BAT using hematoxylin and eosin (H&E) staining showed that the adipocytes from both FACC1KO and WT mice accumulated lipids, this indicated that no defect exists in adipocyte differentiation (Fig. 1*E*). Body composition analyses of 7-week-old male FACC1KO mice compared with WT mice revealed a loss of 16.8% of lean mass (16.4 g vs. 19.7 g, respectively) and a loss of 24% of fat mass (1.9 g vs. 2.5 g, respectively). However, the ratio of either lean mass or fat mass to body weight is not significantly different between the two groups of mice (Fig. 1*F*); this suggests that the differences in total body weight are caused principally by the differences in overall animal size, that is, body length.

Lipogenesis in primary adipocytes from epididymal WAT was analyzed by [^{14}C]-acetate incorporation into the total lipid; no differences were found between FACC1KO and WT mice (Fig. 1*G*). Additions of 100 nM insulin caused a 2.5-fold increase in lipogenesis in both groups, indicating that fatty acid synthesis is not impaired in FACC1KO mice fed a normal diet. Because ACC1 is a rate-limiting enzyme for fatty acid synthesis, this unexpected result may be explained by the inefficient Cre-mediated cleavage of loxP sites. The remaining ACC1 activities may be sufficient for fatty acid synthesis, especially because ACC1 is highly regulated allosterically and by phosphorylation and dephosphorylation.

The fat in adipose tissues comes from two sources, dietary fat and de novo synthesis from dietary carbohydrates. To exclude interference from the dietary fat, we fasted 15- to 16-week-old male mice ($n = 5$) for 2 days to lower fat synthesis; we then fed

them a fat-free diet for 2 days. The mice were killed, and various tissues were isolated and weighed (Fig. 2*A*). The weights of epididymal WAT and intrascapular BAT of FACC1KO mice were 58% less ($P = 0.03$) and 33% less ($P = 0.01$), respectively, than those of WT mice. Because FACC1KO mice are generally smaller than WT mice, the ratio of tissue weight of kidney, liver, and spleen to body weight was not significantly different (Fig. 2*A*). However, the WAT to body weight ratio was 50% less in FACC1KO mice than in WT cohort mice (0.39 ± 0.08% vs. 0.78 ± 0.06%, respectively, $P = 0.01$); the BAT to body weight ratio was only 20% less in FACC1KO mice than in WT mice ($P = 0.08$) (Fig. 2*A*).

The activities of ACC and FAS in both adipose and liver tissue were also measured. Because the amount of fat tissue in individual mutant mice was very low, the fat tissues from five mice were combined and the ACC and FAS activities were measured. In the combined WAT the ACC activity in FACC1KO mice was 50.5% less than that in WT mice. Similarly, in the combined BAT the ACC activity of FACC1KO mice was 66.2% less than that in WT mice (Fig. 2*B*), because the deletion of the ACC1 exon 22 by Cre is less than 85% (Fig. 1*A*), the residual ACC1 activity and the intact activity of ACC2 represented the overall ACC activity observed in the adipose tissues. However, there was a minor reduction, 9.8%, of ACC activity in the liver of FACC1KO mice and no difference in FAS activity was found between FACC1KO and WT mice livers (Fig. 2*C*), suggesting that hepatic FAS was not increased to compensate for the reduction of ACC1 levels in adipose tissue. These results were confirmed by using a group of 18- to 19-week-old female mice ($n = 8$–9) that were treated as described above, and the adipose tissues were pooled for ACC activity measurement. Consistently, the ACC activities in WAT and BAT in FACC1KO mice compared with WT mice were less 64.4% and 57.9%, respectively. ACC activity in the liver of FACC1KO mice compared with WT mice was only 6.5% less. Lower ACC activities lead to a decreased accumulation of lipid in adipose tissues, as shown in the H&E staining (Fig. 2*D*). qRT-PCR analyses of the gene expression in WAT revealed that the ACC1 mRNA level in FACC1KO is only 57% less than WT mice (Fig. 2*E*); this is consistent with the 50.5% lower ACC activities observed in WAT in FACC1KO mice. ACC2 expression is slightly upregulated because it is a minor isoform, less than 10% of the amount of ACC1, and it will contribute minimal ACC activity since its malonyl-CoA is associated with the mitochondrial membrane and does not mix with that generated by ACC1 (4). Other adipocyte differentiation markers such as PPARγ, aP2, and resistin are downregulated only, between 10 and 20% in the WAT of FACC1KO mice. However, when fasted 2 days and re-fed a fat-free diet for 2 days, leptin gene expression is 80% lower in FACC1KO mice than in WT mice (Fig. 2*E*). This reduction in FACC1KO mice compared with WT mice is correlated with the decreased serum leptin level (1,445 ± 153 pg/mL vs. 3,007 ± 391 pg/mL, respectively, $n = 5$, $P = 0.01$).

Reduced Chondrocyte Proliferation and Bone Formation in FACC1KO Mice. To determine whether the growth retardation in FACC1KO mice is caused by a defect in chondrocyte function in the growth plate, we performed a bromodeoxyuridine (BrdU) incorporation assay on the tibia growth plates of the postnatal day 2 and their WT littermates (Fig. 3*A Left*). The data show that BrdU positive chondrocytes in the proliferating zone of the FACC1KO growth plate were about 30% lower than those in the WT littermates (14.45 ± 1.05%, $n = 3$, vs. 20.43 ± 0.88%, $n = 6$, respectively, Fig. 3*A Right*). Dynamic histomorphometry by calcein double staining showed that the bone formation rate was lowered in the FACC1KO mice compared with the WT mice (Fig. 3*B*). These results suggest that decreased proliferation in growth plate chondrocytes causes the shortening of bone elements in the FACC1KO mice.

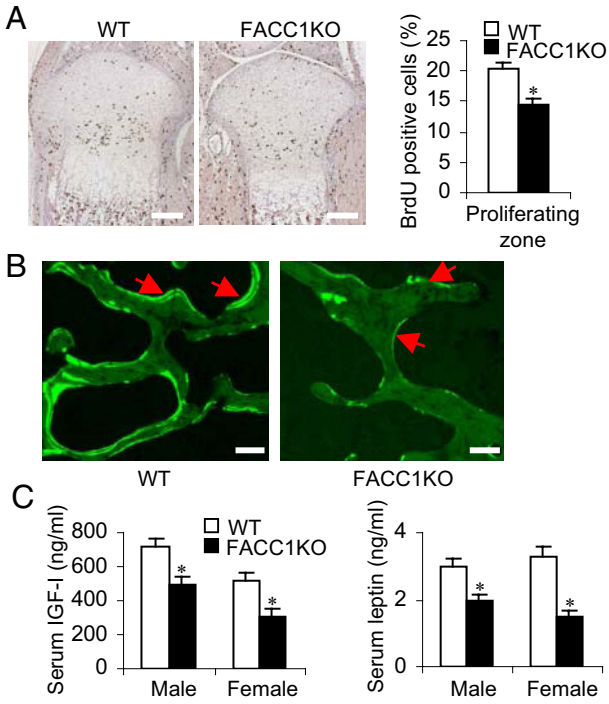

Fig. 3. Reduced chondrocyte proliferation and bone formation in FACC1KO mice. (*A*) Paraffin-embedded nondecalcified sections from tibias of 2-day-old WT mice ($n = 6$) and their FACC1KO littermates ($n = 3$) were immunostained for BrdU. BrdU positive cells have brown nuclei. One representative tibial epiphysis and growth plate from each group is shown (*Left*). BrdU positive chondrocytes in the tibial proliferating zone were counted and percentages are presented for WT mice and FACC1KO mice, respectively (*Right*). *, $P = 0.005$. (*B*) Bone formation rate in vertebrae assessed by double calcein labeling in 3-month-old mice, using formalin-fixed undecalcified 5–7-μm thick plastic sections. (*C*) Analyses of serum IGF1 and leptin levels in 6-week-old mice. For IGF1, $n = 19$ to 24 males or 10 to 12 females; for leptin, $n = 19$ to 24 males or 9 to 12 females. *$P < 0.005$.

Insulin-like growth factor I (IGF1) plays an important role in bone formation. We found that the skeletal phenotype of FACC1KO mice partially phenocopied that of IGF1 knockout mice: short stature, decreased proliferation in growth plate chondrocytes, and lower bone density (12, 13). When we measured the IGF1 level in 6-week-old FACC1KO mice, we found that serum IGF1 levels are reduced by 20% in male mice and 40% in female mice (Fig. 3*C*), suggesting that lowering ACC1 levels in adipose tissue may impact IGF1 production in adipocytes, leading to skeletal dysplasia. However, since the aP2-Cre is expressed also in macrophages and osteoblasts that are derived from the same hematopoietic progenitor cells, we hypothesized that deletion of ACC1 gene in macrophages or osteoblasts may contribute to the bone phenotype in FACC1KO mice. Further investigations are underway to clarify this assumption and determine the molecular mechanism. It is of interest to note that adipose tissue-derived hormone, leptin, with diverse effect as a potent inhibitor of bone formation acting through the central nervous system (14, 15). However, we found that serum leptin level in 6-week-old FACC1KO mice is 35% lower in males and 55% lower in females (Fig. 3*C*). However, at these relatively low levels, leptin did not counteract the osteopenic effect of IGF1. Serum glucose levels of FACC1KO and WT mice are not significantly different, indicating that ACC1KO in the adipose tissues does not affect glucose homeostasis.

Fatty Acid Profile of Bone Lipids. Fatty acid compositions of the total lipids extracted from the tibia/femur of 5-week-old male

mutants and WT male cohort mice were analyzed. The bone of the mutant mice weighed 33% less than WT mice. The fatty acid composition of the lipids, expressed as Mol %, showed that the FACC1KO mutant mice have different compositions than WT mice (Table S1). Saturated fatty acids, C16:0, C18:0, C20:0, C22:0, and C24:0 are 24%, 40%, 15%, 45%, and 45% lower, respectively, in the mutant mice than WT mice. Monounsaturated fatty acids, C16:1, C18:1, and C20:1, are higher while C22:1 and C24:1 are significantly lower in the mutant than WT. The Mol% of linoleic acid, C18:2n-6, and α-linolenic acid, C18:3n-3, the potential precursors of eicosanoids, are significantly higher, 27% and 71%, respectively, in the mutant than WT (Table S1). Arachidonic acid, C20:4n-6, the precursor of prostaglandin E_2 is 35% lower in FACC1KO bone lipids than WT cohort mice.

FACC1KO Mice Show Decreased Osteoblastogenesis. High-resolution X-ray computed tomography (μCT) analyses of lumbar sections of 6-week-old FACC1KO mice revealed mark decreased bone volume with increased medullary cavity space (Fig. 4*A*). This finding is consistent with results from Von Kossa staining of plastic-embedded lumbar vertebrae (Fig. 4*B*). In addition, in FACC1KO mice compared with WT mice, bone histomorphometry showed 36.7% lower trabecular bone volume density (BV/TV) and 26.6% lower trabecular thickness (Tb.Th) in FACC1KO mice compared with WT mice, (Fig. 4*C*). Combined and cooperative activities of osteoblasts (for bone formation) and osteoclasts (for bone resorption) determine the impact on the bone architecture (16). Toluidine blue staining on the plastic-embedded slides of 6-week-old mouse vertebrae L5 showed fewer osteoblasts in FACC1KO mice compared with WT cohort mice, that is, 44.1% less for osteoblast surface per bone surface, Ob.S/BS, and 41.1% less for number of osteoblasts per bone perimeter, N.Ob/B.Pm, (Fig. 4 *D* and *F*). Then new trabecular bones extended from the hypertrophic zone of growth plate had the most active bone formation activity. In this area of the WT samples, the active osteoblasts arrays covered the majority of the trabecular surface (Fig. 4*D*, red line denotes covered surfaces). However, in the same area of the FACC1KO samples, far fewer osteoblast surfaces are covered (Fig. 4*D*). In contrast, tartrate-resistant acid phosphatase, TRAP, staining revealed that the osteoclast number was not significantly different between FACC1KO and WT mice (Fig. 4 *E* and *F*).

In the 5-day-old FACC1KO pups, RT-PCR analyses of total RNA from isolated osteoblasts revealed that ACC1 exon 22 is deleted in the osteoblasts; this is also confirmed by PCR analyses of genomic DNA from calvaria which show the deletion of the ACC1 gene (Fig. 4*G*). Furthermore, qRT-PCR analyses showed expression in the calvaria of some osteoblast differentiation markers (17)—such as α1 (I) collagen; Alp, alkaline phosphatase; osteocalcin; Runx2; IGFBP5, IGF1 binding protein 5; BMP2, bone morphogenic protein 2; and osteopontin were down regulated (Fig. 4*H*)—which confirmed that the aP2-Cre-mediated ACC1 deletion modulates osteoblast differentiation and/or formation. These results indicate that ACC1 plays an important role in osteoblast formation or differentiation in FACC1KO mice, and that a decreased number of osteoblasts appear to be the major cause of osteopenia and prenatal growth retardation.

ACC1 has been thought to be a good target for the drug treatment of obesity (18, 19). To test whether the disruption of ACC1 in adipose tissues would inhibit diet-induced obesity, 2-month-old male mice were fed a high fat/high carbohydrate (HF/HC) diet for 10 weeks. The FACC1KO mice which weighed less at the beginning of the HF/HC diet, gained as much weight as WT cohort mice, and they eventually became obese. There were no differences between FACC1KO and WT mice in blood parameters of glucose, TG and cholesterol. Oil red O staining of liver sections showed overloaded lipid in both groups. These data suggest that aP2-Cre-mediated inactivation of ACC1 in adipose tissue could not prevent diet-induced obesity and hepatic steatosis.

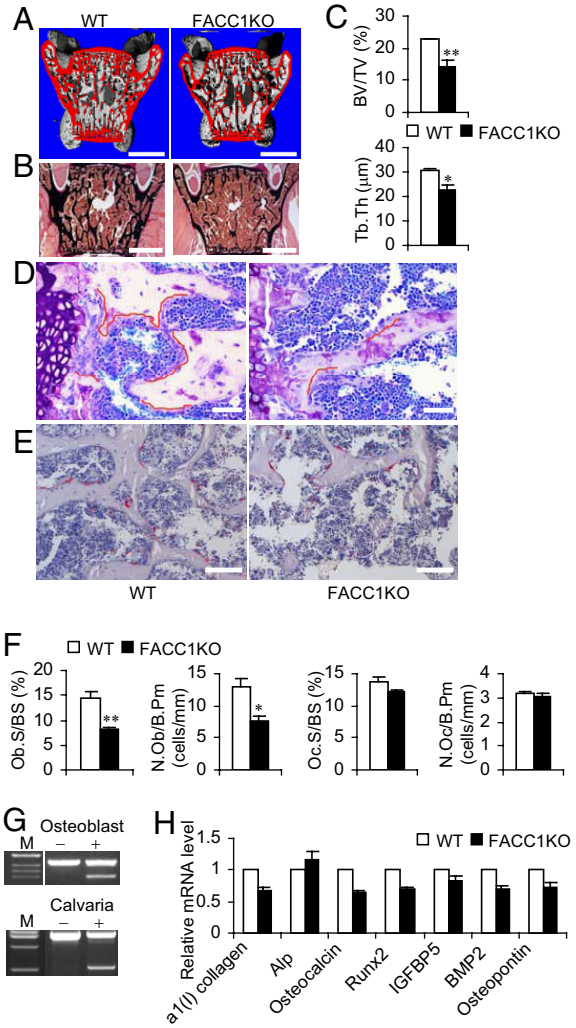

Fig. 4. Effect of ACC1 on osteoblastogenesis. (*A*) Representative μCT image of lumbar sections (spine elements L5) from 6-week-old WT and FACC1KO mice. The surfaces of cortical and trabecular bones are shown in red. (Scale bar, 1 mm.) (*B*) Von Kossa staining of lumbar sections of 6-week-old mice. (Scale bar, 1 mm.) (*C*) Analyses of trabecular bone density (BV/TV) and trabecular thickness (Tb.Th) of 6-week-old mice (n = 3–4). *, $P < 0.05$; **, $P < 0.005$. (*D*) Toluidine blue staining of lumbar sections of 6-week-old mice. (Scale bar, 50 μm.) (*E*) TRAP staining of lumbar sections of 6-week-old mice. (Scale bar, 100 μm.) (*F*) Histomorphometric analyses of spine trabecular bone of 6-week-old mice. Ob.S./BS, osteoblast surface per bone surface; N.Ob/B.Pm, number of osteoblasts per bone perimeter; Oc.S./BS, osteoclast surface per bone surface; N.Oc/B.Pm, number of osteoclasts per bone perimeter. *$P < 0.05$; ** $P < 0.01$. (*G*) RT-PCR analyses of total RNA from osteoblasts using primers 21f/24r (*Left*). Genomic DNA from calvaria was analyzed using primers flanking upstream (forward) and downstream (reverse) loxP sites (3). The lower bands represent the deletion of exon 22 in the ACC1 gene. The minus and plus signals represent the absence and presence of Cre, respectively. (*H*) qRT-PCR analyses of total RNA from 6-week-old mouse calvaria (n = 4). Alp, alkaline phosphatase; IGFBP5, IGF1 binding protein 5; BMP2, bone morphogenic protein 2.

Discussion

ACC1 knockout mice, FACC1KO, were generated by intercrossing aP2-Cre transgenic mice with $ACC1^{lox/lox}$ mice. aP2 is expressed predominantly in adipose, cartilage tissue, vertebrae, and macrophage (20–22). Under lipogenic conditions of fasting/re-feeding fat-free diet, knockout of ACC1 in WAT and BAT led

to decreased ACC activities and decreased accumulation of lipid as compared with WT mice. However, a HF/HC diet induced obesity and hepatic steatosis in both FACC1KO mice and WT mice, indicating that inactivation of ACC1 does not prevent diet-induced obesity. This finding can be explained by the incompleteness of the Cre-mediated excision of the ACC1 gene; the remaining ACC activities are enough to trigger fatty acid synthesis, especially since ACC1 is highly regulated allosterically by and phosphorylation.

Interestingly, the FACC1KO mice showed prenatal growth retardation and weighed less after birth; this was accompanied by decreased chondrocyte proliferation in the growth plate and associated with lower trabecular bone density. Bone growth and homoeostasis is achieved by modeling and remodeling that are carried out by primary skeletal cell types—chondrocytes, osteoblasts, and osteoclasts—which are responsible for the formation of cartilage and bone (16). These cells are influenced by many regulatory hormones and molecules. Interruption in their regulations lead to impaired bone homeostasis which results in different bone diseases (16). FACC1KO mice showed decreased amounts of serum IGF1 and leptin (Fig. 3*C*). IGF1 has two important functions in prenatal and postnatal skeletal development. First, IGF1 is essential for the embryonic development of bone; it regulates and coordinates chondrocyte proliferation, maturation, and apoptosis to form endochondral bones of appropriate sizes and strengths (12). IGF1 deficiency in mice resulted in markedly reduced chondrocyte proliferation, severe dwarfism of the axial and appendicular skeleton, and reduced mineralization of the spinal column (12). Second, IGF1 is required for normal embryonic and postnatal growth in mice (22–24). Compared with their WT littermates, heterozygous ($IGF1^{+/-}$) mice have 37% lower levels of IGF1, and they are 10–20% smaller. The lower level of serum IGF1, the small skeleton size, the shortened long bone lengths, and the lower chondrocyte proliferating rate of FACC1KO mice all mimic the phenotype of IGF1 knockout mice. It is interesting that earlier studies showed that liver-specific IGF1 deletion resulted in 75% lower circulating IGF1 but did not affect the overall growth of these mice (25, 26). The discrepancies between our study results and the results of the liver IGF1 specific deletion studies may be explained by development stages of the deletion—results of either the timing or cell type of the deletions. The albumin-Cre are expressed relatively later during development, while aP2-Cre is expressed at very early stages during embryonic development leading to growth retardation in FACC1KO mice. Moreover, because the ACC1 deletion occurs within bone, a potential paracrine effect cannot be ruled out. Leptin, which is expressed and secreted from adipocytes, plays an important role in regulating the energy expenditure, body weight, and bone mass in animals (27–29). In addition, it negatively regulates osteoblasts and the formation of bones through a hypothalamic relay (15, 30). Inactivation of ACC1 in FACC1KO mice led to decreased serum leptin, which is consistent with the previous report that ACC inhibitor benzafibrate decreased leptin release from primary adipocytes (31). It is of interest to note that the decreased leptin levels in FACC1KO mice could not overcome decreased IGF1 levels; possibly because of its relatively decreased levels of about 30–50%, which may not be low enough to reverse IGF1 effects. Alternatively, loss of ACC1 in osteoblastic tissues caused a cell autonomous effect that could not be overcome by upstream signaling.

We found that ACC1 is also mutated in the osteoblast of FACC1KO mice and several osteoblast-specific markers were downregulated (Fig. 4*G*). The relatively lower ACC1 in osteoblasts might have affected the synthesis and the chain elongation of fatty acids especially those of the very long chain fatty acids; as shown by the relatively lower Mol% of C20 homolog and higher Mol% of their precursors linoleic and linolenic acids in the FACC1KO mutant compared to their WT cohorts (Table S1). The number of the osteoblast cells was reduced and their specific marker genes such as a1 (I) collagen, Runx2, and osteocalcin were downregulated in the mouse calvaria, indicating that ACC1 exerts its regulation directly on osteoblastogenesis. The decreased number of osteoblasts may have a major effect on bone formation in FACC1KO mice. This study provides evidence that ACC1, a lipogenic enzyme, has a direct impact on bone homeostasis.

Recently, Karsenty and coworkers have established a link between bone and energy metabolism (32). They discovered that bone is an important organ, which endocrinally regulates energy metabolism. Adipose-derived hormone leptin regulates the bone formation (15), and reciprocally bone regulates glucose homeostasis and fat metabolism through bone-specific hormone osteocalcin (32). Deficiency of osteocalcin exhibited abnormally high amount of visceral fat. We found the gene expression of osteocalcin in the bone of FACC1KO mice was lower, but the glucose homeostasis and adiposity were not changed. This discrepancy probably is due to the low efficiency of aP-Cre and ACC1 activities were not completely abolished in osteoblasts or adipose tissues.

Finally, ACC1 and its isoform ACC2 have become pharmaceutical targets, of concern for the inhibition of lipid accumulation and the prevention of hepatic steatosis and obesity (18, 19). Present results showed that inactivation of ACC1could not protect the mice against diet-induced obesity or hepatic steatosis. Instead, the interruption of the function of ACC1 resulted in bone defects that need to be considered in targeting the carboxylase. ACC2 knockout mice have been shown to be a good model for the inhibition of lipid accumulation in liver or adipose tissue through continuous fatty acid oxidation (4); therefore, the development of a selective inhibitor to ACC2 appears to be a viable approach for identifying a pharmacological product targeting diet-induced obesity and diabetes (33).

Materials and Methods

Animals. Mice C57BL/6J and transgenic mice expressing Cre recombinase under control of rat aP2 promoter (aP2-Cre mice) were purchased from The Jackson Laboratory (16). The generation of C57/BL/6J mice containing the floxed ACC1 allele were bred with aP2-Cre to generate aP2-Cre^{+}/$ACC1^{lox/lox}$ mice, thereafter referred to as FACC1KO mice. Mice were fed a regular diet (PicoLab 5053) or, when indicated, a fat free diet (MP Biomedicals, catalog no. 901683) or a HF/HC diet (Bioserv, catalog no. F3282) (3).

Analyses of ACC1 and FAS Activities in Liver and Adipose Tissues. Liver, epididymal WAT, and interscapular BAT tissues resected from mice were snap frozen and ground to powder in liquid nitrogen. The powdered tissues were suspended as previously described (34, 35), and suspended tissues were homogenized using Polytron and the extracts were centrifuged at 35,000 × *g* for 20 min. The supernatant fluid was treated with ammonium sulfate to 45% saturation, and the precipitated proteins were collected by centrifugation (60,000 × *g* for 30 min) and dissolved in a buffer containing 50 mM HEPES (pH 7.5), 0.1 mM DTT, 1 mM EDTA, and 10% glycerol. The suspensions were clarified by centrifugation and assayed for ACC and FAS activities (36, 37).

Blood Metabolite Assays. Measurement of glucose and β-hydroxybutyrate (ketone) levels in whole blood, and insulin, TG, cholesterol, and NEFA levels in serum samples were performed (3). Serum leptin and IGF1 levels were measured using mouse leptin ELISA kit (Crystal Chem Inc.), and mouse IGF1 EIA kit (Diagnostic Systems Laboratories) according to the manufacturers' instructions.

Body Composition. Dual-energy x-ray absorptiometry was used to measure fat body mass and lean body mass components in live mice. Mice used for X-ray absorptiometry were anesthetized and scanned two times with a Lunar PIXImus densitometer.

Histology for Liver and Adipose Tissues. Adipose tissues were fixed in 10% neutral buffered formalin and embedded in paraffin, and 5–8-μm sections were cut and stained with hematoxylin and eosin. Livers frozen in Tissue-Tek OCT (Sakura Finetek) were stained with Oil Red O to identify the neutral lipids.

Lipogenesis Assay. Adipocytes were isolated from the pooled epididymal fat pads of 4-month-old male WT mice and FACC1KO mice following tissue digestion with collagenase type II (Sigma) (37). Adipocytes (2×10^5 cells) were resuspended in 1 mL Krebs-Ringer-bicarbonate HEPES (KRBH) buffer containing 4% (wt/vol) fatty acid-free BSA fraction V (Sigma), 3 mM glucose, 0.5 mM acetate, and 1 μCi [1-^{14}C] acetate (56 mCi/mmol, MP Biochemicals) in either the absence or the presence of 100 nM insulin at 37 °C for 2 h under 95% O_2-5% CO_2. The reactions were terminated by adding 40 μL 10 N H_2SO4, and the ^{14}C incorporation into lipids was determined (38).

Bromodeoxyuridine (BrdU) Incorporation. For the proliferating study, 2-day-old FACC1KO pups and their WT littermates were injected i.p. with 20 μL BrdU (Zymed); 90 min following injection, the pups were killed by decapitation and the femoral and tibial joints of the hindlimbs were dissected, fixed in 4% paraformaldehyde overnight, and embedded in paraffin. Five-μm sections were deparaffinized and stained with a BrdU detection kit (Zymed). The nuclei were counterstained with hematoxylin. BrdU-positive nuclei and total nuclei numbers in the proliferating zone of the tibia growth plate were counted with the automeasurement module of Zeiss Axiovision software.

Skeletal Analysis, Histomorphometry, and Calcein Labeling. Skeletons from 7-day-old mice were prepared and stained with alcian blue for cartilage and with alizarin red for calcified tissues (12). Using standard protocols, toluidine blue, TRAP, and Von Kossa stainings were performed on 5- to 7-μm thick undecalcified lumbar vertebral plastic sections. Double labeling was performed by i.p. calcein (Sigma) injection twice, with an interval of 4 days. Mice were killed 2 days following the second injection. Calcein labeling was assessed in the vertebrae using formalin-fixed undecalcified 5- to 7-μm thick plastic sections (39). μCT scanning of lumbar spine from 6-week-old mice was performed in formalin-fixed sections with a μCT scanner (GE Healthcare).

RT-PCR and qRT-PCR. The RNA was isolated from various tissues—liver, adipose, bone marrow, tibia, and calvaria—or from primary cells such as osteoblasts (40) and peritoneal macrophages (41). The RNA was reverse transcribed to cDNA and analyzed by PCR using ACC1 primers 21f (5′-GTCTGCTGGGAAGTTAATCCAG-3′) and 24r (5′-TCCTGCAGCTCTAGCAGAGG-3′), located in exons 21 and 24, respectively. For qRT-PCR analysis, the total RNA was treated with DNase and quantified (3). The primer sequences are available upon request.

Gas Chromatography Analyses of Fatty Acid Profiles in Bone. Long femur and tibia bones were dissected free of surrounding tissues, and homogenized in PBS buffer containing 40 mM EDTA (pH 8.0). The lipid was extracted and analyzed (42). The compositions of each fatty acid are expressed as Mol%.

Statistical Analyses. Data are expressed as mean value ± standard error of the mean (SEM). Statistical comparisons were performed using unpaired, two-tailed Student's *t* test. A difference was considered as significant when $P < 0.05$.

ACKNOWLEDGMENTS. We thank Dr. Kenneth Ellis, Angela Major, and Vijayalakshmi Nannegari for assistance and Dr. Lutfi Abu-Elheiga for discussion and comments. This work is supported by National Institutes of Health Grant GM-63115 (to S.J.W.), the Hefni Tech Training Foundation, and the Medallion Foundation.

1. Wakil SJ, Stoops JK, Joshi VC (1983) Fatty acid synthesis and its regulation. *Annu Rev Biochem* 52:537–579.
2. Abu-Elheiga L, et al. (2005) Mutant mice lacking acetyl-CoA carboxylase 1 are embryonically lethal. *Proc Natl Acad Sci USA* 102:12011–12016.
3. Mao J, et al. (2006) Liver-specific deletion of acetyl-CoA carboxylase 1 reduces hepatic triglyceride accumulation without affecting glucose homeostasis. *Proc Natl Acad Sci USA* 103:8552–8557.
4. Abu-Elheiga L, Matzuk MM, Abo-Hashema KA, Wakil SJ (2001) Continuous fatty acid oxidation and reduced fat storage in mice lacking acetyl-CoA carboxylase 2. *Science* 291:2613–2616.
5. Ahima RS, Flier JS (2000) Adipose tissue as an endocrine organ. *Trends Endocrinol Metab* 11:327–332.
6. He W, et al. (2003) Adipose-specific peroxisome proliferator-activated receptor gamma knockout causes insulin resistance in fat and liver but not in muscle. *Proc Natl Acad Sci USA* 100:15712–15717.
7. Kim KH (1997) Regulation of mammalian acetyl-coenzyme A carboxylase. *Annu Rev Nutr* 17:77–99.
8. Garbay B, Bauxis-Lagrave S, Boiron-Sargueil F, Elson G, Cassagne C (1997) Acetyl-CoA carboxylase gene expression in the developing mouse brain. Comparison with other genes involved in lipid biosynthesis. *Brain Res Dev Brain Res* 98:197–203.
9. Mao J, Marcos S, Davis SK, Burzlaff J, Seyfert HM (2001) Genomic distribution of three promoters of the bovine gene encoding acetyl-CoA carboxylase alpha and evidence that the nutritionally regulated promoter I contains a repressive element different from that in rat. *Biochem J* 358:127–135.
10. Barber MC, Travers MT (1995) Cloning and characterisation of multiple acetyl-CoA carboxylase transcripts in ovine adipose tissue. *Gene* 154:271–275.
11. Mao J, Chirala SS, Wakil SJ (2003) Human acetyl-CoA carboxylase 1 gene: Presence of three promoters and heterogeneity at the 5′-untranslated mRNA region. *Proc Natl Acad Sci USA* 100:7515–7520.
12. Wang Y, et al. (2006) Insulin-like growth factor-I is essential for embryonic bone development. *Endocrinology* 147:4753–4761.
13. Wang Y, et al. (2006) Role of IGF-I signaling in regulating osteoclastogenesis. *J Bone Miner Res* 21:1350–1358.
14. Zhang Y, et al. (1994) Positional cloning of the mouse obese gene and its human homologue. *Nature* 372:425–432.
15. Ducy P, et al. (2000) Leptin inhibits bone formation through a hypothalamic relay: A central control of bone mass. *Cell* 100:197–207.
16. Watkins BA, Lippman HE, Le Bouteiller L, Li Y, Seifert MF (2001) Bioactive fatty acids: Role in bone biology and bone cell function. *Prog Lipid Res* 40:125–148.
17. Yamaguchi A, Komori T, Suda T (2000) Regulation of osteoblast differentiation mediated by bone morphogenetic proteins, hedgehogs, and Cbfa1. *Endocr Rev* 21:393–411.
18. Harwood HJ, Jr (2005) Treating the metabolic syndrome: Acetyl-CoA carboxylase inhibition. *Expert Opin Ther Targets* 9:267–281.
19. Tong L (2005) Acetyl-coenzyme A carboxylase: Crucial metabolic enzyme and attractive target for drug discovery. *Cell Mol Life Sci* 62:1784–1803.
20. Urs S, Harrington A, Liaw L, Small D (2006) Selective expression of an aP2/fatty acid binding protein 4-Cre transgene in non-adipogenic tissues during embryonic development. *Transgenic Res* 15:647–653.
21. Maeda K, et al. (2005) Adipocyte/macrophage fatty acid binding proteins control integrated metabolic responses in obesity and diabetes. *Cell Metab* 1:107–119.
22. Baker J, Liu JP, Robertson EJ, Efstratiadis A (1993) Role of insulin-like growth factors in embryonic and postnatal growth. *Cell* 75:73–82.
23. Powell-Braxton L, et al. (1993) IGF-I is required for normal embryonic growth in mice. *Genes Dev* 7:2609–2617.
24. Lupu F, Terwilliger JD, Lee K, Segre GV, Efstratiadis A (2001) Roles of growth hormone and insulin-like growth factor 1 in mouse postnatal growth. *Dev Biol* 229:141–162.
25. Liu JL, Yakar S, LeRoith D (2000) Mice deficient in liver production of insulin-like growth factor I display sexual dimorphism in growth hormone-stimulated postnatal growth. *Endocrinology* 141:4436–4441.
26. Sjogren K, et al. (1999) Liver-derived insulin-like growth factor I (IGF-I) is the principal source of IGF-I in blood but is not required for postnatal body growth in mice. *Proc Natl Acad Sci USA* 96:7088–7092.
27. Friedman JM, Halaas JL (1998) Leptin and the regulation of body weight in mammals. *Nature* 395:763–770.
28. Ahima RS, Flier JS (2000) Leptin. *Annu Rev Physiol* 62:413–437.
29. Badman MK, Flier JS (2007) The adipocyte as an active participant in energy balance and metabolism. *Gastroenterology* 132:2103–2115.
30. Elefteriou F, et al. (2004) Serum leptin level is a regulator of bone mass. *Proc Natl Acad Sci USA* 101:3258–3263.
31. Shirai Y, Yaku S, Suzuki M (2004) Metabolic regulation of leptin production in adipocytes: A role of fatty acid synthesis intermediates. *J Nutr Biochem* 15:651–656.
32. Lee NK, et al. (2007) Endocrine regulation of energy metabolism by the skeleton. *Cell* 130:456–469.
33. Xu X, et al. (2007) The synthesis and structure-activity relationship studies of selective acetyl-CoA carboxylase inhibitors containing 4-(thiazol-5-yl)but-3-yn-2-amino motif: Polar region modifications. *Bioorg Med Chem Lett* 17:1803–1807.
34. Thampy KG, Wakil SJ (1988) Regulation of acetyl-coenzyme A carboxylase. I. Purification and properties of two forms of acetyl-coenzyme A carboxylase from rat liver. *J Biol Chem* 263:6447–6453.
35. Brink J, et al. (2002) Quaternary structure of human fatty acid synthase by electron cryomicroscopy. *Proc Natl Acad Sci USA* 99:138–143.
36. Thampy KG, Wakil SJ (1985) Activation of acetyl-CoA carboxylase. Purification and properties of a Mn2+-dependent phosphatase. *J Biol Chem* 260:6318–6323.
37. Arslanian MJ, Wakil SJ (1975) Fatty acid synthase from chicken liver. *Methods Enzymol* 35:59–65.
38. Rodbell M (1964) Metabolism of isolated fat cells. I. Effects of hormones on glucose metabolism And lipolysis. *J Biol Chem* 239:375–380.
39. Engin F, et al. (2008) Dimorphic effects of Notch signaling in bone homeostasis. *Nat Med* 14:299–305.
40. Ducy P, et al. (1999) A Cbfa1-dependent genetic pathway controls bone formation beyond embryonic development. *Genes Dev* 13:1025–1036.
41. Murtaugh MP, et al. (1983) Induction of tissue transglutaminase in mouse peritoneal macrophages. *J Biol Chem* 258:11074–11081.
42. Chang BH, et al. (2006) Protection against fatty liver but normal adipogenesis in mice lacking adipose differentiation-related protein. *Mol Cell Biol* 26:1063–1076.